



Identification of tumor antigens for mRNA vaccines and ferroptosis-related landscape in esophageal squamous cell carcinoma

Qin Zeng, Bo Chen, Wei Wang

Department of Radiation Oncology, Nanfang Hospital, Southern Medical University, Guangzhou, China

Contributions: (I) Conception and design: W Wang; (II) Administrative support: W Wang; (III) Provision of study materials or patients: Q Zeng; (IV) Collection and assembly of data: Q Zeng, B Chen; (V) Data analysis and interpretation: Q Zeng, B Chen; (VI) Manuscript writing: All authors; (VII) Final approval of manuscript: All authors.

Correspondence to: Bo Chen, MD, MM; Wei Wang, MD, PhD. Department of Radiation Oncology, Nanfang Hospital, Southern Medical University, Baiyun District, Shatai Road, Guangzhou 510515, China. Email: helen866909@163.com; wwei9500@smu.edu.cn.

Background: Ferroptosis, an iron-dependent form of cell death that is characterized by lipid peroxidation, has been implicated in conferring resistance to cancer therapies and may contribute to the pathogenesis of esophageal squamous cell carcinoma (ESCC). Furthermore, messenger RNA (mRNA) vaccines have emerged as a promising modality in the treatment arsenal against diverse malignancies. The aim of the study was to investigate the role of ferroptosis subtypes in ESCC and the immune microenvironment, as well as to identify key genes that could serve as targets for mRNA vaccine development.

Methods: Gene expression profiles and clinical data from 79 and 358 ESCC patients were collected from The Cancer Genome Atlas and Gene Expression Omnibus databases. Subsequently, we identified tumor mutational burden (TMB), immune microenvironment scores, and immune checkpoint and immune cell dysfunction genes for each ferroptosis subtype. Furthermore, we utilized weighted gene co-expression network analysis (WGCNA) to describe the immune landscape of ESCC and identify key genes for mRNA vaccine development.

Results: Our analysis revealed that *MMD*, *MTDH*, and *TRFC* were overexpressed ferroptosis genes in ESCC. In addition, ESCC was categorized into two ferroptosis subtypes, namely FS1 and FS2. Notably, FS2 exhibited a poorer prognosis, higher TMB, and increased immune cell infiltration when compared to FS1. The ferroptosis landscape analysis further revealed the presence of three distinct states. WGCNA analysis identified different modules of interest emerging as an independent prognostic factor and enriched with hub genes that could serve as targets for mRNA vaccine development.

Conclusions: The ferroptosis subtypes demonstrated significant associations with both prognosis and the immune microenvironment in ESCC. Additionally, the module of interest identified through immune landscape analysis represented an independent prognostic factor, with its contained genome offering promising targets for mRNA vaccine development.

Keywords: Ferroptosis; esophageal squamous cell carcinoma (ESCC); messenger RNA vaccine (mRNA vaccine); immunotherapy

Submitted Nov 01, 2023. Accepted for publication Apr 28, 2024. Published online Jun 20, 2024.

doi: 10.21037/tcr-23-2027

View this article at: <https://dx.doi.org/10.21037/tcr-23-2027>

Introduction

Esophageal cancer is a significant global health concern, ranking seventh in terms of new incidence and sixth in terms

of mortality. The 5-year survival rate for this malignancy is alarmingly low, ranging from 15–25% (1,2). Geographically, the incidence of esophageal cancer exhibits considerable variation worldwide, with approximately half of all cases

occurring in China (1). This disease encompasses two primary pathological types: esophageal squamous cell carcinomas (ESCCs) and esophageal adenocarcinomas, with the former comprising over 90% of cases in China (3,4). Despite advancements in current therapeutic modalities such as surgery, radiotherapy, chemotherapy, and immunotherapy, there has been limited improvement in the prognosis of ESCC patients (5,6). Consequently, efforts are being focused on the exploration of more effective treatment options.

Ferroptosis is a form of programmed cell death characterized by the excessive iron-dependent peroxidation of lipids, leading to the accumulation of lipid peroxides and reactive oxygen species (ROS) (7,8), which constitutes a key mechanism of action for certain anti-tumor drugs (9). The alterations of ROS contribute to evading cell death, promoting cell proliferation, remodeling the tumor microenvironment, and facilitating local and metastatic spread (10,11). Thus, the dysregulation of ferroptosis pathways plays a crucial role in the development of resistance to cancer treatment. Core components involved in the ferroptosis-associated signaling pathways include glutathione (*GSH*), glutathione peroxidase 4 (*GPX4*), and solute carrier family 7 member 11 (*SLC7A11*) (12). Inhibitors of *GPX4*, such as *RSL3* and *ML-162*, have been shown to induce ferroptosis in head and neck squamous

cell carcinoma cells, while artemisinin (*ART*) can induce ferroptosis in tumor cells by depleting *GSH* and increasing ROS accumulation (13). Additionally, inhibiting *SLC7A1* has been found to enhance the response to ferroptosis in cancer cell growth (14). Nevertheless, the mechanisms underlying the involvement of ferroptosis in ESCC development and anti-cancer therapy remain unclear.

Tumor immunotherapy has emerged as a cornerstone in the field of cancer therapeutics. Therapeutic tumor vaccines, especially messenger RNA (mRNA) vaccines, have unequivocally demonstrated clinical efficacy across multiple cancer types (15,16). mRNA vaccines facilitate the delivery of specific mRNA sequences containing encoded protein information, thereby instructing the synthesis of target proteins within the body. This mechanism ultimately triggers a tailored immune response, contributing to the treatment and prevention of various diseases. Importantly, mRNA vaccines bypass the need for comprehensive whole-genome DNA profiling, minimizing concerns related to gene insertions or deletions. Moreover, mRNA vaccines elicit robust and enduring immune responses, further enhancing their efficacy (17,18). However, there is a lack of extracted and purified tumor-specific antigens (TSA) that are exclusively present in tumor cells but absent in normal cells and tissues. Current mRNA vaccines primarily focus on tumor-associated antigens (TAA), which limits the specificity and effectiveness of these vaccines. Therefore, it is crucial to identify specific TSA to facilitate the development of mRNA vaccines. In our study, our objective is to investigate the role of ferroptosis in ESCC and assess its association with the antitumor effectiveness and prognosis of the specific population. Furthermore, by identifying specific antigens and elucidating the landscape of ferroptosis in ESCC, we tried to establish a solid theoretical foundation for the advancement of mRNA vaccines. We present this article in accordance with the TRIPOD reporting checklist (available at <https://tcr.amegroups.com/article/view/10.21037/tcr-23-2027/rc>).

Methods

Data source

The RNA sequencing data, specifically in fragments per kilobase of transcript per million mapped reads (FPKM) and Count formats, along with the clinical data from The Cancer Genome Atlas (TCGA)-ESCC cohorts (n=251), were downloaded from the UCSC Xena database (<https://>

Highlight box

Key findings

- Two distinct ferroptosis subtypes were identified within esophageal squamous cell carcinoma (ESCC) patient profiles. Furthermore, gene expression analysis has unveiled the upregulation of specific ferroptosis-associated genes in ESCC, presenting potential targets for the development of messenger RNA (mRNA) vaccine therapies.

What is known and what is new?

- Ferroptosis plays a role in cancer development and resistance to therapies. mRNA vaccines have also been recognized as effective against various cancers.
- The discovery of potential hub genes that could be utilized for mRNA vaccine development is a novel finding.

What is the implication, and what should change now?

- The implication of these findings is that targeting ferroptosis pathways and related gene expressions could lead to new therapeutic strategies in treating ESCC. Considering the prognostic value of the identified gene modules, the clinical practice may start to incorporate ferroptosis-related gene expression profiling as a standard to aid in the risk assessment.

xena.ucsc.edu/). Somatic mutation statistics were extracted from 184 ESCC patients using the maftools R package. To strengthen the findings obtained from TCGA database, gene expression and clinical data from the GSE53625 cohort were downloaded from the Gene Expression Omnibus (GEO) database. Out of the 358 samples in the GSE53625 dataset, 179 ESCC samples with comprehensive survival information were included in our study. To identify ferroptosis-related genes, including driver genes, suppressors, and markers, we obtained relevant information from the FerrDb database, resulting in a collection of 424 ferroptosis-related genes. Additionally, we sourced immune cell death (ICD) and immune checkpoint (ICP) genes from relevant literature to enrich our analysis. The study was conducted in accordance with the Declaration of Helsinki (as revised in 2013). The current study follows the open-source TCGA and GEO data access policies and publication guidelines. Data can be downloaded for free. There are no ethical issues and informed consent in our study was not required.

Overexpressed genes and mutation screening

In the TCGA-ESCC cohort, we employed the DESeq2 package to identify differential expression genes (DEGs) between normal and malignant esophagus samples. The cutoff criteria used were $|\log_2\text{fold change}| > 1$ and a P value < 0.05 . DEGs with a $\log_2\text{fold change} > 0$ or < 0 were categorized as highly expressed or lowly expressed, respectively. Furthermore, we utilized the Gene Set Cancer Analysis (GSCA) database (<http://bioinfo.life.hust.edu.cn/GSCA/#/>) for analyzing potential tumor antigens, specifically analyzing single nucleotide variations (SNVs) and copy number variations (CNVs). The GSCA database is an online analysis tool designed to study cancer, drugs, and immunological genomics.

Tumor antigens and immune cell infiltration

To examine the correlation between potential tumor antigens and antigen-presenting cells (APCs), we employed the MCPcounter method to assess the infiltration of immune cells and stromal cells within the tumors. The MCPcounter method provides estimates for the abundance of eight immune cell populations, including CD4⁺ T cells, CD8⁺ T cells, natural killer (NK) cells, B lymphocytes, monocytes, dendritic cells, neutrophils, and cytotoxic lymphocytes (which encompasses CD8⁺ T cells and cytotoxic innate lymphoid cells, NK cells). To determine the relationship between the abundance

estimates and potential tumor antigen gene expression, we performed Spearman correlation analyses. A P value below 0.05 was considered statistically significant, indicating a meaningful correlation between the abundance of immune cells/stromal cells and the expression of potential tumor antigen genes.

Identification and validation of ferroptosis-related subtypes

To investigate the expression profiles of ferroptosis-related genes, we utilized the “ConsensusClusterPlus” R package. This approach involved clustering the genes based on their expression patterns, generating consensus matrices, and identifying distinct subtypes related to ferroptosis. To obtain robust results, we performed 1,000 replicates, where each replicate involved resampling 80% of the patients in the cohort. The genetic cluster (K) number was varied between 2 and 9 to explore different potential subtypes. To determine the optimal K-clusters, we evaluated the cumulative density function (CDF) and consensus matrix. These assessments helped in selecting the most appropriate number of clusters that best represented the underlying subtypes related to ferroptosis. Additionally, we applied the same settings to an independent data set (GSE53625) and assessed if the subtypes showed consistent patterns across different datasets. This validation step helped ensure the robustness and reproducibility of the identified ferroptosis-related subtypes.

Prognostic significance of ferroptosis-related subtypes

The prognostic significance of ferroptosis-related subtypes was assessed utilizing the log-rank test. The relationships between ferroptosis subtypes and ferroptosis-associated molecules and cellular features were further investigated. The Chi-square test was employed to select the most frequently mutated genes. To ascertain the immune enrichment score of each sample, single-sample Gene Set Enrichment Analysis (ssGSEA) from the GSVA package was implemented. To visualize the distribution of ferroptosis-related subtypes in patients, we employed graph learning-based dimensionality reduction analysis and used the R package Monocle with a Gaussian distribution. The maximum number of components (N) was set to 4, and we applied the discriminative dimensionality reduction with trees (DDRTree) method.

Gene co-expression network

We performed screening of immune-related gene modules

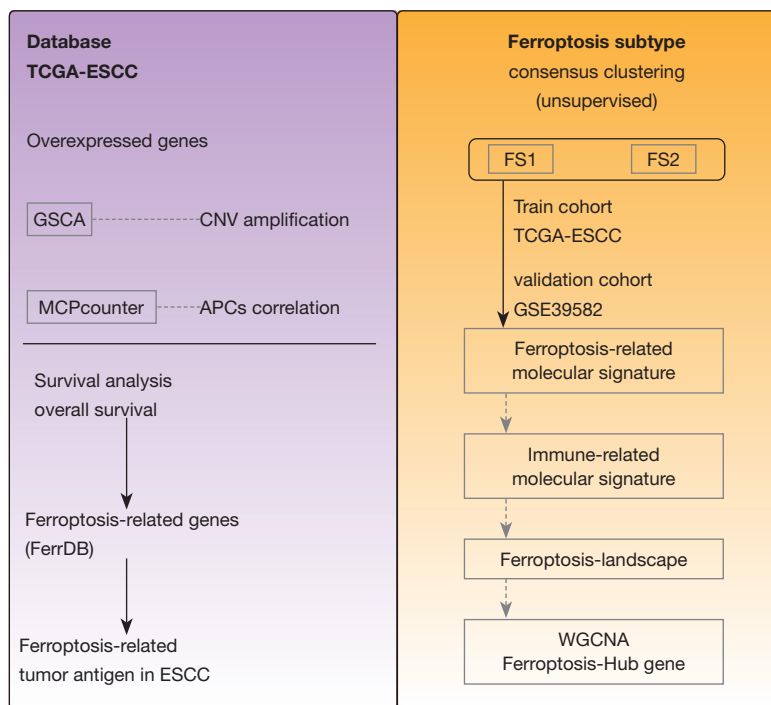


Figure 1 A flowchart of this study. TCGA, The Cancer Genome Atlas; ESCC, esophageal squamous cell carcinoma; GSCA, Gene Set Cancer Analysis; CNV, copy number variation; APC, adenomatous polyposis coli; FS1, ferroptosis subtype 1; FS2, ferroptosis subtype 2; WGCNA, weighted gene co-expression network analysis.

using the “WGCNA” package. The soft-thresholding power (β) was determined, and we found that 6 was the optimal value to construct a scale-free co-expression network. Next, a topological matrix was created, followed by hierarchical clustering, with module eigengenes calculated. The inter-module correlation was assessed based on module eigengenes, and hierarchical clustering was performed. For functional enrichment analysis, we utilized the Metascape database (www.metascape.org/), which included Kyoto Encyclopedia of Genes and Genomes (KEGG) and Gene Ontology (GO) analyses.

Statistical analysis

All statistical analyses were conducted using R (version 4.2.0). Comparisons between two groups were assessed using the Mann-Whitney *U* test, while comparisons between more than two groups were performed using the Kruskal-Wallis test. The Spearman rank correlation method was utilized for correlation analysis. A threshold of $P=0.05$ was considered statistically significant.

Results

Identifying potential ferroptosis-related antigens in ESCC

Figure 1 provides an overview of our study. In this study, we detected a total of 9,862 DEGs to identify potential tumor antigens for ESCC. Among these DEGs, 5,836 genes were found to be possibly overexpressed and encoding tumor antigens (Figure 2A). To identify potential tumor antigens with the properties suitable for mRNA vaccines, we performed a screening process that involved assessing the interaction with APCs and considering the prognostic data of overexpressed genes. We also examined genes with amplified copy numbers. As a result, three genes, namely *MMD*, *MTDH*, and *TFRC*, were found to be associated with ferroptosis and qualified as potential tumor antigens (Figure 2B). Further analysis comparing ESCC and normal tissue revealed that *MMD*, *MTDH*, and *TFRC* exhibited significantly higher expression in ESCC compared to normal tissues (Figure 2C-2E). Additionally, the CNV analysis indicated that these three genes had significant copy number amplification (Figure 2F-2H). Correlation

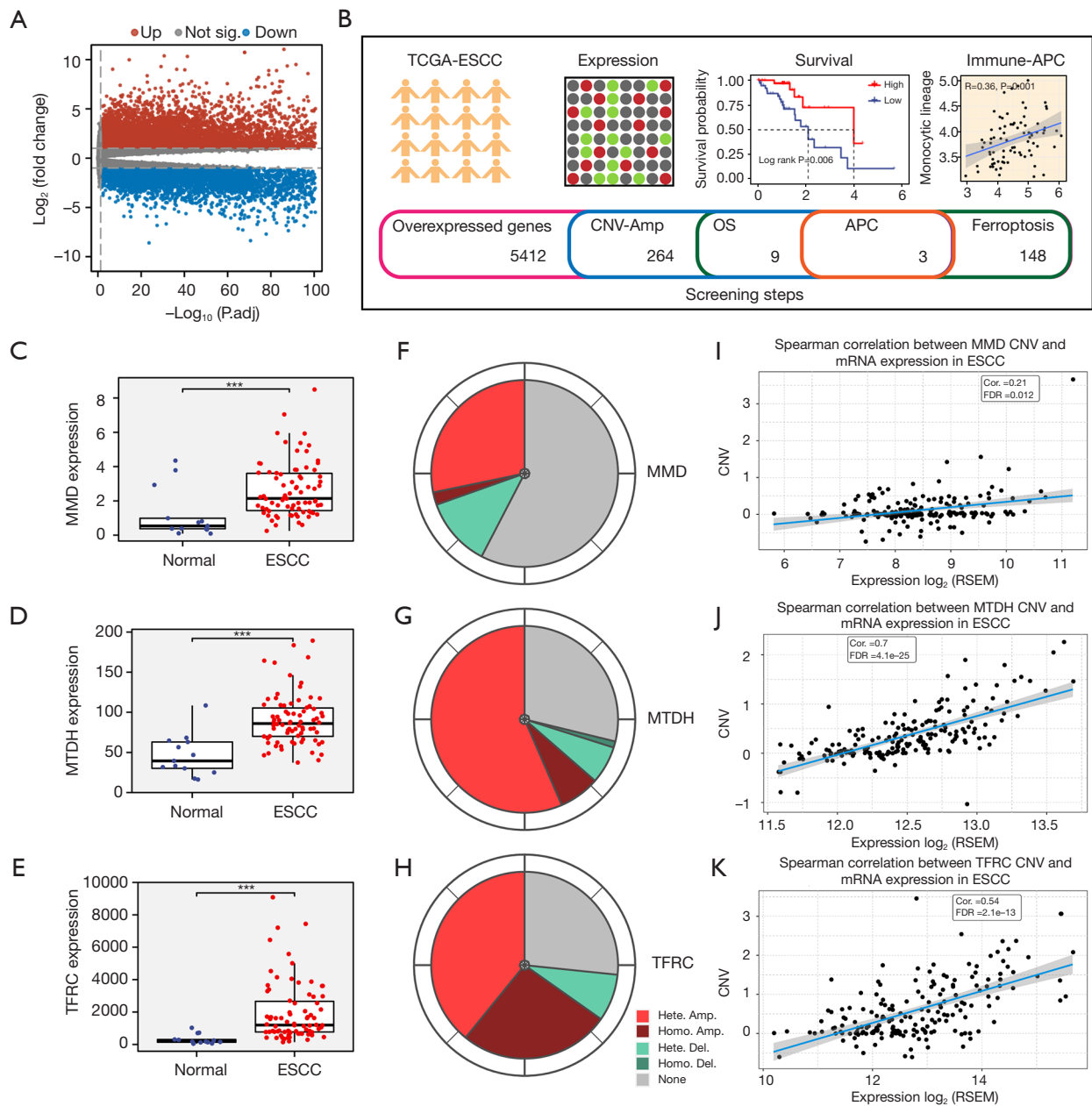


Figure 2 The identification of potential anti-tumor antigens in ESCC. (A) A volcano plot compared the expression of normal to tumor esophagus tissues in the TCGA-ESCC database. (B) The screening flow of the potential antigens of ESCC. (C-E) The different expression of *MMD*, *MTDH* and *TFRC* in normal and tumor tissues. (F-H) The copy number variation of *MMD*, *MTDH* and *TFRC*. (I-K) The correlation analysis between the gene expression of *MMD*, *MTDH* and *TFRC* and copy number variation. ***, $P < 0.001$. Not sig., not significant; TCGA, The Cancer Genome Atlas; ESCC, esophageal squamous cell carcinoma; APC, adenomatous polyposis coli; CNV, copy number variation; Amp, amplification; OS, overall survival; Hete., heterozygous; Homo., homozygous; Del., deletion; ESCC, esophageal squamous cell carcinoma; Cor., correlation; FDR, false discovery rate; RSEM, RNA-Seq by Expectation-Maximization.

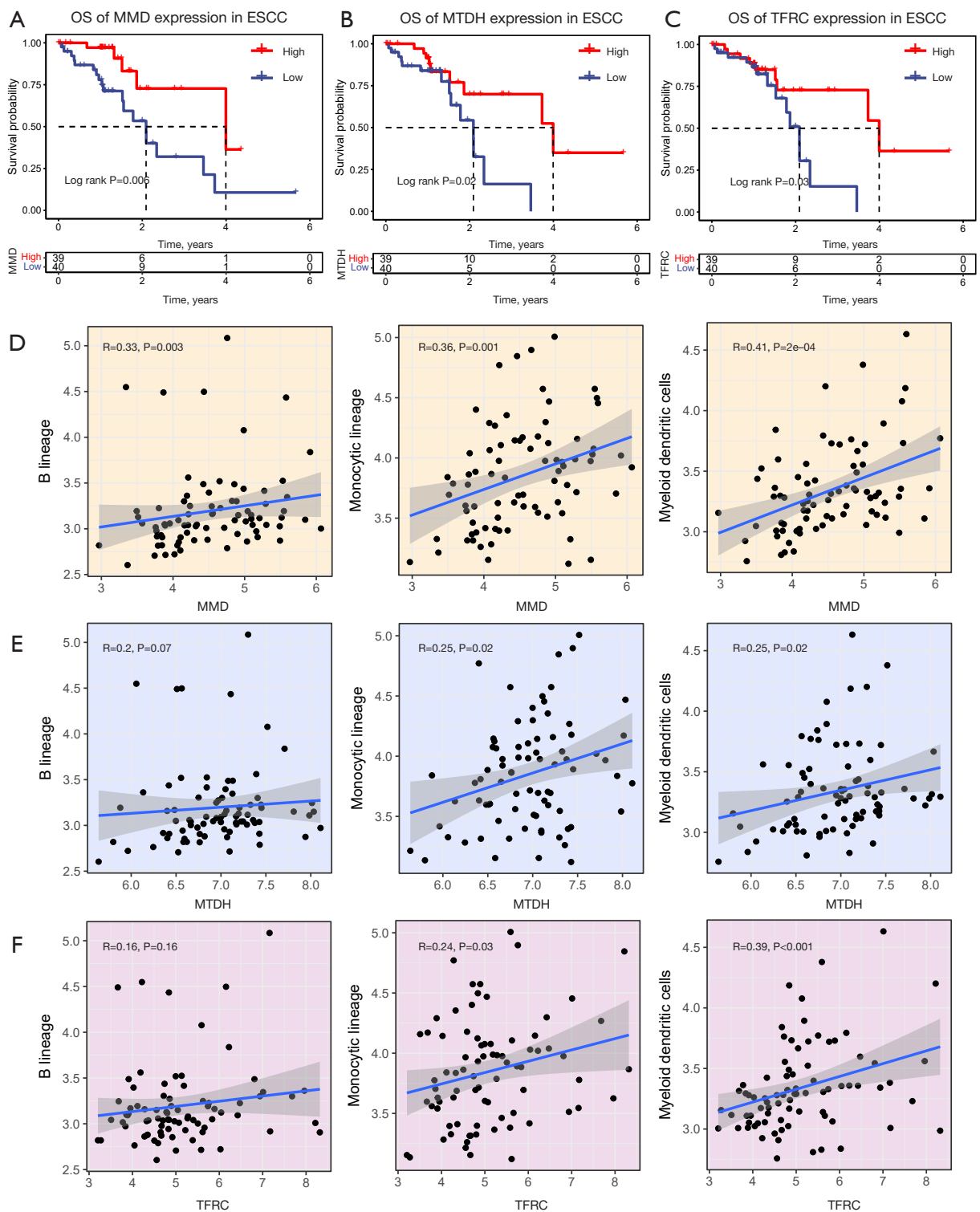


Figure 3 The identification of prognosis-associated tumor neoantigens. (A-C) Kaplan-Meier curves of OS of ESCC patients. (D-F) Correlation was analysed between MMD, MTDH and TFRC and antigen-presenting cells. OS, overall survival; ESCC, esophageal squamous cell carcinoma.

analysis between CNV and gene expression demonstrated a significant positive relationship, particularly for *MTDH* and *TFRC* (Figure 2I-2K). Overall, these findings identify *MMD*, *MTDH*, and *TFRC* as potential tumor antigens for ESCC, as they were overexpressed in ESCC tissue, exhibited significant copy number amplification, and showed a positive correlation between CNV and gene expression.

Prognostic value of ferroptosis-related DEGs

Patients with high expression of *MMD*, *MTDH*, and *TFRC* genes experienced significantly more favorable prognoses compared to those with low gene expression (Figure 3A-3C). Additionally, we explored the correlation between these three genes and APC. MCPcounter method with correlation analysis demonstrated a significant positive relationship between the *MMD* gene and B cells, macrophages, and dendritic cells (Figure 3D). *MTDH* and *TFRC* were significantly positively associated with macrophages and dendritic cells (Figure 3E, 3F). Overall, APCs were shown to be likely involved in the direct processing of tumor antigens, their presentation to T cells, and subsequent immune response. Furthermore, these genes may induce ferroptosis in tumor cells, leading to their elimination.

Identification of potential ferroptosis-related subtypes in ESCC

Ferroptosis, a critical mechanism for eliminating tumor cells, has been shown to have a close relationship with tumor immunity. Typifying the different manifestations of ferroptosis within tumors and the tumor microenvironment can aid in the identification of patients suitable for vaccination. Therefore, we sought to examine the expression profile of 424 genes associated with ferroptosis in TCGA-ESCC data, allowing us to construct consensus clusters. Through the utilization of CDF and the area under the CDF curve (Figure 4A, 4B), we determined a suitable *k* value of 2. Subsequently, the ferroptosis-related genes were divided into two stable clusters, named FS1 and FS2 (Figure 4C). Furthermore, principal component analysis (PCA) demonstrated a significant distinction between these two ferroptosis-related subtypes (Figure 4D). This observation was consistent in the GSE53625 cohort, where it also displayed two distinct ferroptosis subtypes, FS1 and FS2 (Figure 4E). Prognostic analysis indicated that within the TCGA-ESCC cohort, FS1 displayed a closer

association with favorable prognosis, while FS2 exhibited a lower survival rate (Figure 4F). Similarly, in the GSE53625 cohort, FS1 also displayed superior prognoses compared to FS2 (Figure 4G). These findings highlight consistent discrepancies in survival outcomes between TCGA-ESCC and GSE53625 cohorts. Furthermore, observations across different time periods revealed an irregular distribution of the two ferroptosis subtypes. Specifically, within the TCGA-ESCC dataset, all patients in stage IV belonged to the FS2 subtype, while FS1 and FS2 had comparable proportions among stage III-IV patients. In the GSE53625 dataset, the proportion of FS2-type patients was higher than that of FS1-type patients among individuals in the intermediate or late stages (Figure 4H, 4I). In summary, the characterization of ferroptosis subtypes has the potential to predict the prognoses of patients with ESCC, as evidenced by the validation across different cohorts.

Associations between ferroptosis-related subtype, mutation status and immunomodulators

Elevated tumor mutation burden (TMB) and somatic mutation rate are indicative of enhanced antitumor immunity. Initially, TMB and the total number of mutations in each patient with ESCC were ascertained by evaluating TCGA-ESCC mutation data in relation to ferroptosis subtypes. Notably, the FS2 subtype exhibited significantly higher TMB and total mutation numbers compared to the FS1 subtype ($P < 0.05$), as illustrated in Figure S1A, S1B. Furthermore, analysis of 30 genes revealed varying mutation statuses in the two subtypes, encompassing *TP53*, *TTN*, *KMT2D*, *NFE2L2*, *CSMD3*, *MUC16*, *NOTCH1*, among others (Figure S1C). In conclusion, FS2-type patients display a propensity towards heightened genomic instability and robust antitumor immunity. TMB holds potential as an indicator for potential application of mRNA-based ferroptosis vaccines.

Previous research has demonstrated the crucial roles played by ICPs such as *PD-L1* and *TIM-3*, as well as ICD regulators including *CALR* and *HMGB1*, in modulating the immune response against tumors, thereby influencing the effectiveness of mRNA vaccines. Additionally, there exists a correlation between ferroptosis and immunoregulation. Hence, we undertook an assessment of the differential expression of ICPs and ICD regulators in two distinct ferroptosis subtypes. In the TCGA-ESCC cohort, we identified a total of 25 ICD genes, of which 20 displayed differential expression between the two subtypes. In the

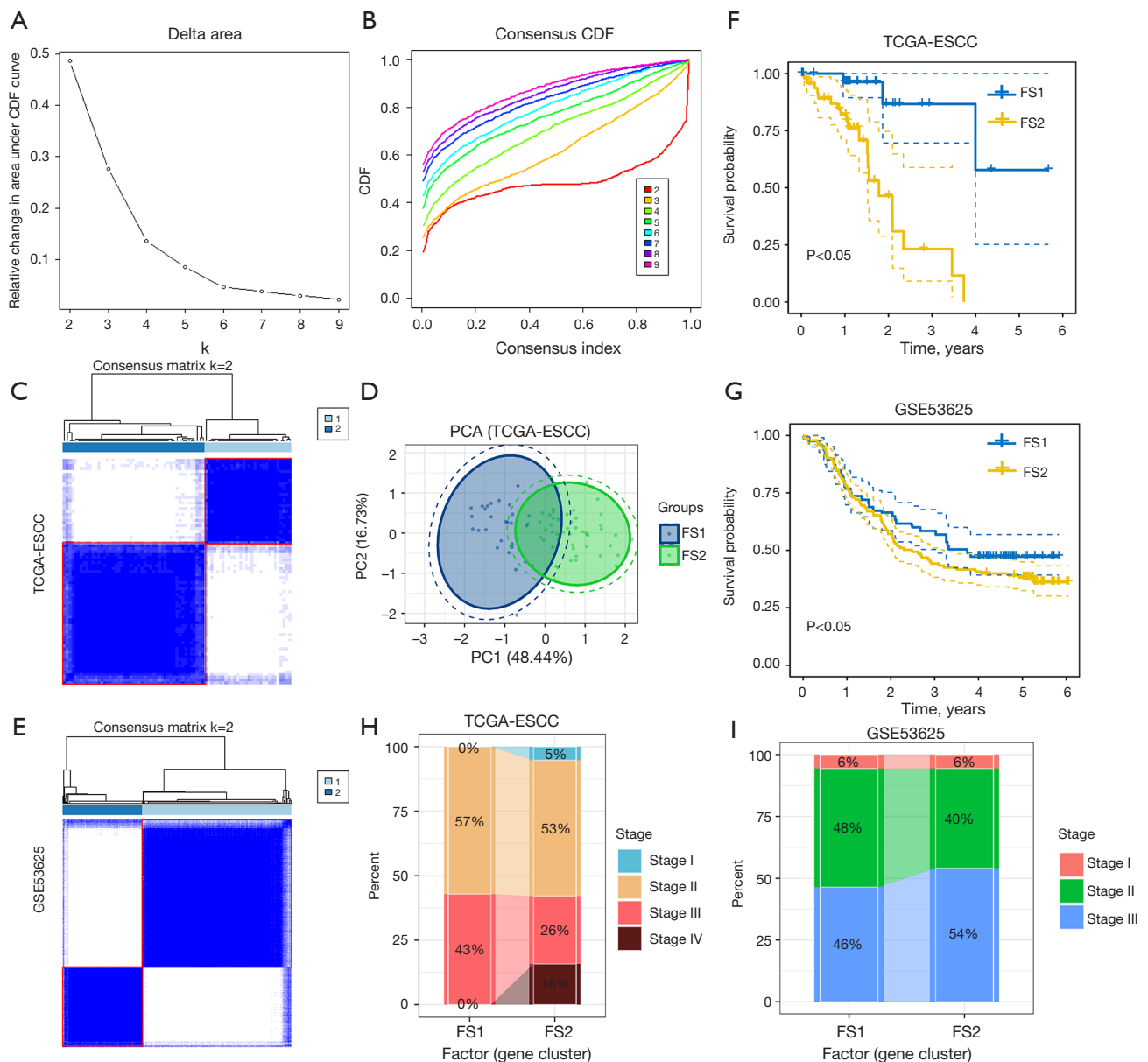


Figure 4 Ascertain of possible ferroptosis subtype. (A,B) Delta area curve (A) and cumulative distribution function curve (B) of ferroptosis corresponding genes in TCGA-ESCC. (C) The two ferroptosis-related clusters based on TCGA-ESCC. (D) Principal component analyses of ferroptosis subtypes in TCGA-ESCC. (E) The two ferroptosis-related clusters based on GSE53625. (F,G) Kaplan-Meier curve of OS of the ferroptosis subtypes in TCGA (F) and GSE53625 (G). (H,I) Distribution of TNM stage of different ferroptosis subtypes of ESCC patients. CDF, cumulative density function; TCGA, The Cancer Genome Atlas; ESCC, esophageal squamous cell carcinoma; FS1, ferroptosis subtype 1; FS2, ferroptosis subtype 2; PCA, principal component analysis; PC, principal component; OS, overall survival; TNM, tumor-node-metastasis.

GSE53625 cohort, 12 ICD genes were identified, and 8 of them exhibited differential expression between the subtypes. Notably, the differentially expressed ICDs exhibited similar trends in expression across the different subtypes, with *EIF2K2*

and *LRP1* being downregulated in FS2 (Figure 5A,5B). While several molecules did not demonstrate statistically significant differences in expression, most ICD genes displayed similar trends in both datasets. Furthermore, we

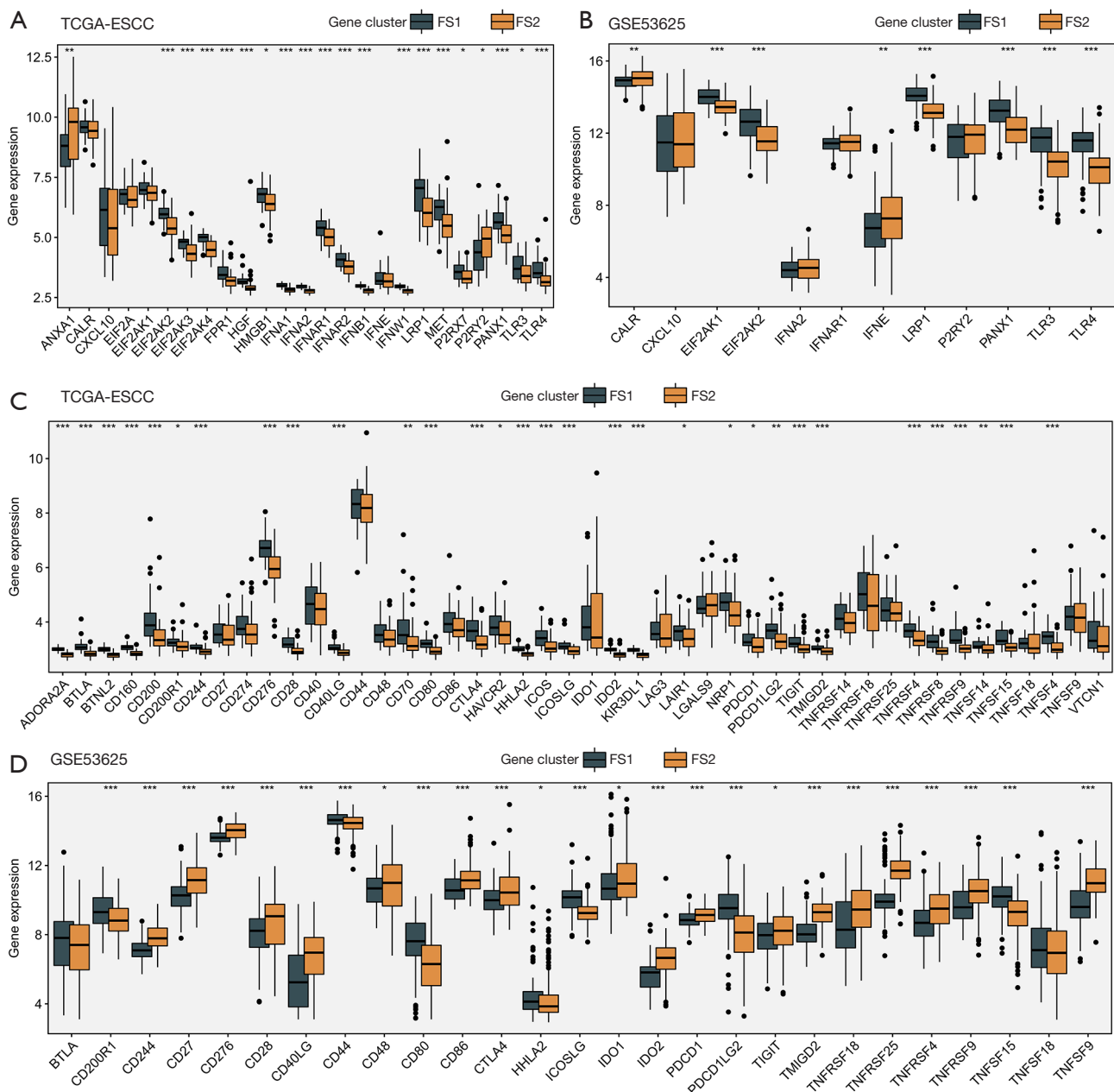


Figure 5 The correlation between ferroptosis subtypes and the regulated genes of ICD or ICP. The differential expression of ICD in FS1 and FS2 of ESCC in TCGA (A) or GSE53625 (B) cohort, respectively. (C,D) The variant expression of ICP in FS1 and FS2 of ESCC in TCGA (C) or GSE53625 (D) cohort, respectively. *, $P < 0.05$; **, $P < 0.01$; ***, $P < 0.001$. TCGA, The Cancer Genome Atlas; ESCC, esophageal squamous cell carcinoma; FS1, ferroptosis subtype 1; FS2, ferroptosis subtype 2; ICD, immune cell death; ICP, immune checkpoint.

confirmed the presence of 46 ICP genes in the TCGA-ESCC cohort, with 31 of them displaying differential expression between the subtypes. In the GSE53625 cohort, 27 ICP genes were identified, and 25 of them exhibited

differential expression between the subtypes (Figure 5C,5D). The expression trends of ICP genes were found to be similar in both cohorts. Overall, the expression levels of ICD regulators and ICPs in ferroptosis subtypes may act as

biomarkers for mRNA vaccines. It is possible that mRNA vaccination may exhibit enhanced efficacy in patients with upregulated ICD regulators, while patients with high ICP expression may display reduced efficacy.

Molecular features of ferroptosis-related subtypes

The response to mRNA vaccines is contingent upon the immune status of tumors. We employed ssGSEA to assess 28 previously reported signature gene sets from the TCGA-ESCC and GSE53625 cohorts, in order to further delineate the immune cell components within the two ferroptosis subtypes. Notably, these subtypes exhibited substantially distinct immune cell compositions (Figure 6A,6B), with elevated scores indicating more immune cell infiltration in FS2 patients. Our KM analysis divulged significant variations in the prognosis of 28 immune cell types, including activated CD8 T cells, CD56 bright NK cells, CD56 dim NK cells, and NK cells, based on high and low scores. Higher scores were indicative of worse prognoses (Figure 6C). Moreover, employing the ESTIMATE algorithm, we observed increased immune cell infiltration in FS2 patients, as compared to FS1 patients, within the TCGA-ESCC and GSE53625 cohorts. Additionally, FS1 counterparts displayed higher ESTIMATE and stromal scores relative to FS2 individuals (Figure 6D,6E). Collectively, these findings suggest that FS2 may exemplify an immune hot phenotype, whereas FS1 may represent an immune cold phenotype. Consequently, ferroptosis subtypes hold the potential to reflect the immunological status in ESCC patients, thereby facilitating the identification of individuals suitable for mRNA vaccination.

Ferroptosis landscape in ESCC

The construction of a ferroptosis map using the expression profile of ferroptosis-related genes allowed us to divide ESCC patients into three trajectories (Figure 7A). The transverse axis (PCA1) was found to be positively correlated with multiple immune cells such as type 17 T helper cells, plasmacytoid dendritic cells, neutrophils, and immature dendritic cells (Figure 7B). However, there was no significant association between the longitudinal axis (PCA2) and the 28 types of immune signatures. Interestingly, within the same ferroptosis subtype, we observed heterogeneity among the samples (Figure 7C). Based on the trajectory positions, we assigned all samples to three states, and their proportions varied across different ferroptosis subtypes

(Figure 7D). Prognosis analysis showed differences in survival curves among the three states, but the curves did not exhibit significant discrimination (Figure 7E).

Co-expression modules of ferroptosis-related hub genes

The identification of immune-related hub genes can be valuable in confirming the eligibility of patients for mRNA vaccines. In our study, we employed a WGCNA to identify these hub genes. We set β to 4, resulting in a scale-free network (Figure 8A). To achieve this, we transformed the gene expression matrix into an adjacency matrix. Subsequently, we established genetic modules, each containing a minimum of 20 genes. The eigengene values of each module were calculated, and modules exhibiting high similarity were merged. Ultimately, we obtained four distinct modules, with any unassigned genes placed in the grey module (Figure 8B,8C). Comparing the module eigengene values, we discovered that FS1 exhibited significantly higher values than FS2 in both the turquoise and brown modules (Figure 8D). Kaplan-Meier curves were utilized to evaluate the prognostic significance of these modules. Notably, only the turquoise module displayed a significant difference in prognosis based on high and low values. Higher values in the turquoise module were associated with better prognoses (Figure 8E). Subsequently, we conducted a multivariate Cox analysis on the module eigengene values to identify modules capable of independently predicting prognosis (Figure 8F). Furthermore, we performed functional enrichment analysis on genes within the turquoise module. This analysis revealed a predominant enrichment of genes related to NK cell-mediated cytotoxicity, response to bacterium, and positive regulation of response to external stimulus (Figure S2; table available at <https://cdn.amegroups.com/static/public/tcr-23-2027-1.pdf>). Therefore, hub genes identified through our analysis hold potential as biomarkers for predicting the prognoses of ESCC patients and selecting appropriate candidates for mRNA vaccination.

Discussion

The present study embarked on a comprehensive analysis with the explicit goal of pinpointing the interrelationship between ferroptosis and prognosis in ESCC. By assiduously filtering through massive datasets from TCGA and GEO, we identified a subset of genes that hold therapeutic promise in crafting mRNA vaccines tailored to ESCC. Delving deeper, we implemented clustering methodologies

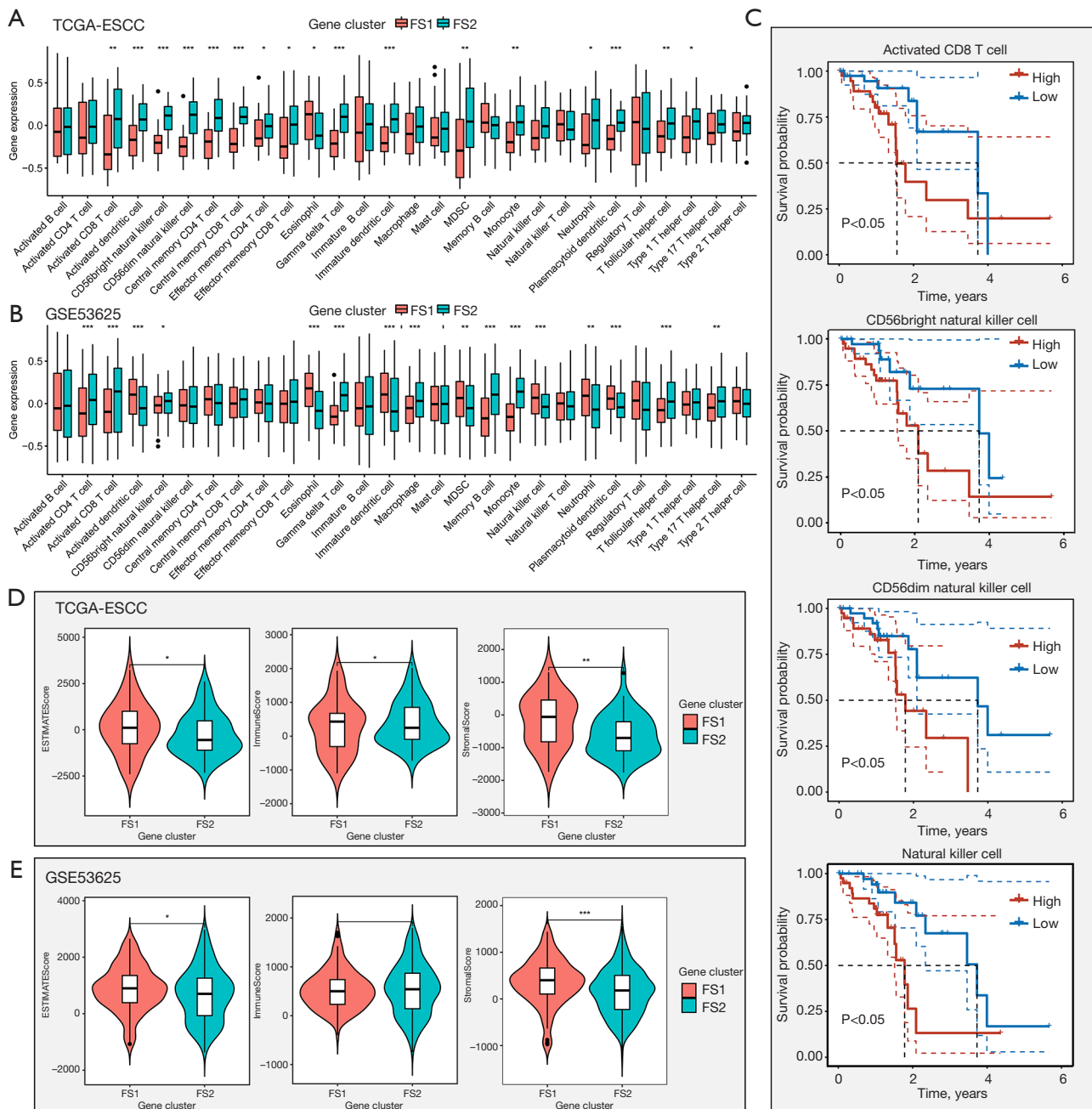


Figure 6 ssGSEA of 28 kinds of immune cells in ferroptosis subtypes. (A,B) The difference risk score of 28 immune cell types in different ferroptosis subtype in TCGA (A) and GSE53625 (B). (C) Kaplan-Meier of high or low risk subgroup of activated CD8 T cell, CD56 bright natural killer cell, CD56 dim natural killer cell and natural killer cell in TCGA-ESCC. (D,E) The comparison of ESTIMATE score, immune score and stromal score in TCGA-ESCC (D) and GSE53625 (E). *, $P < 0.05$; **, $P < 0.01$; ***, $P < 0.001$. TCGA, The Cancer Genome Atlas; ESCC, esophageal squamous cell carcinoma; MDSC, myeloid-derived suppressor cell; FS1, ferroptosis subtype 1; FS2, ferroptosis subtype 2; ssGSEA, single-sample Gene Set Enrichment Analysis.

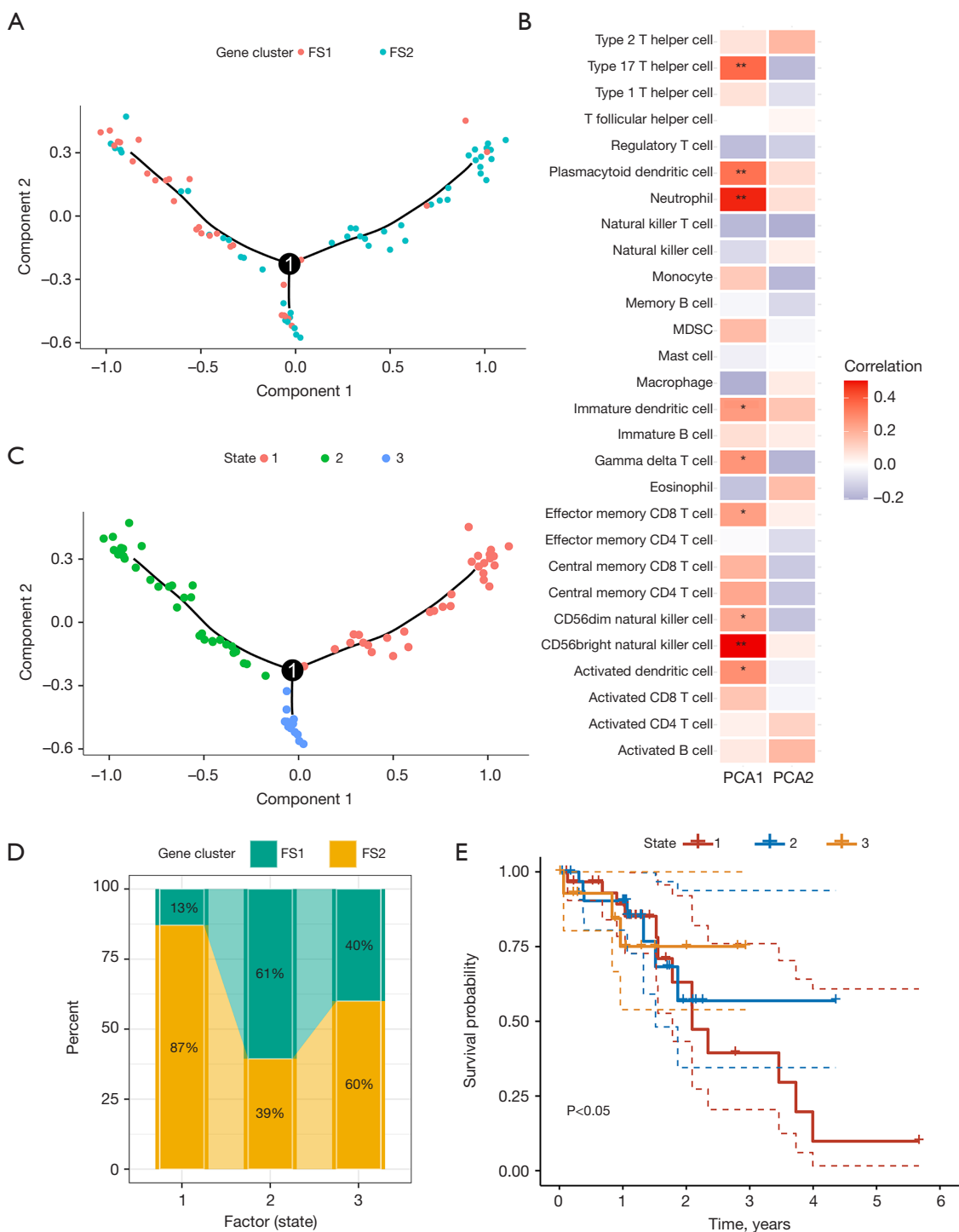


Figure 7 The landscape of ferroptosis in ESCC. (A) Landscape of each ESCC patients. The location and color of each patient in immunogram correspond to the subtypes of ferroptosis, representing the overall characteristics of FRME. (B) Correlations of PCA1/2 and immune cells modules. (C) Each ESCC patients was reclassified according to their position to state 1,2,3. (D) The proportion of different ferroptosis subtypes of patients in the top state. (E) Kaplan-Meier survival analysis of different state patients. *, P<0.05; **, P<0.01. MDSC, myeloid-derived suppressor cell; FS1, ferroptosis subtype 1; FS2, ferroptosis subtype 2; ESCC, esophageal squamous cell carcinoma; FRME, ferroptosis-related microenvironment; PCA, principal component analysis.

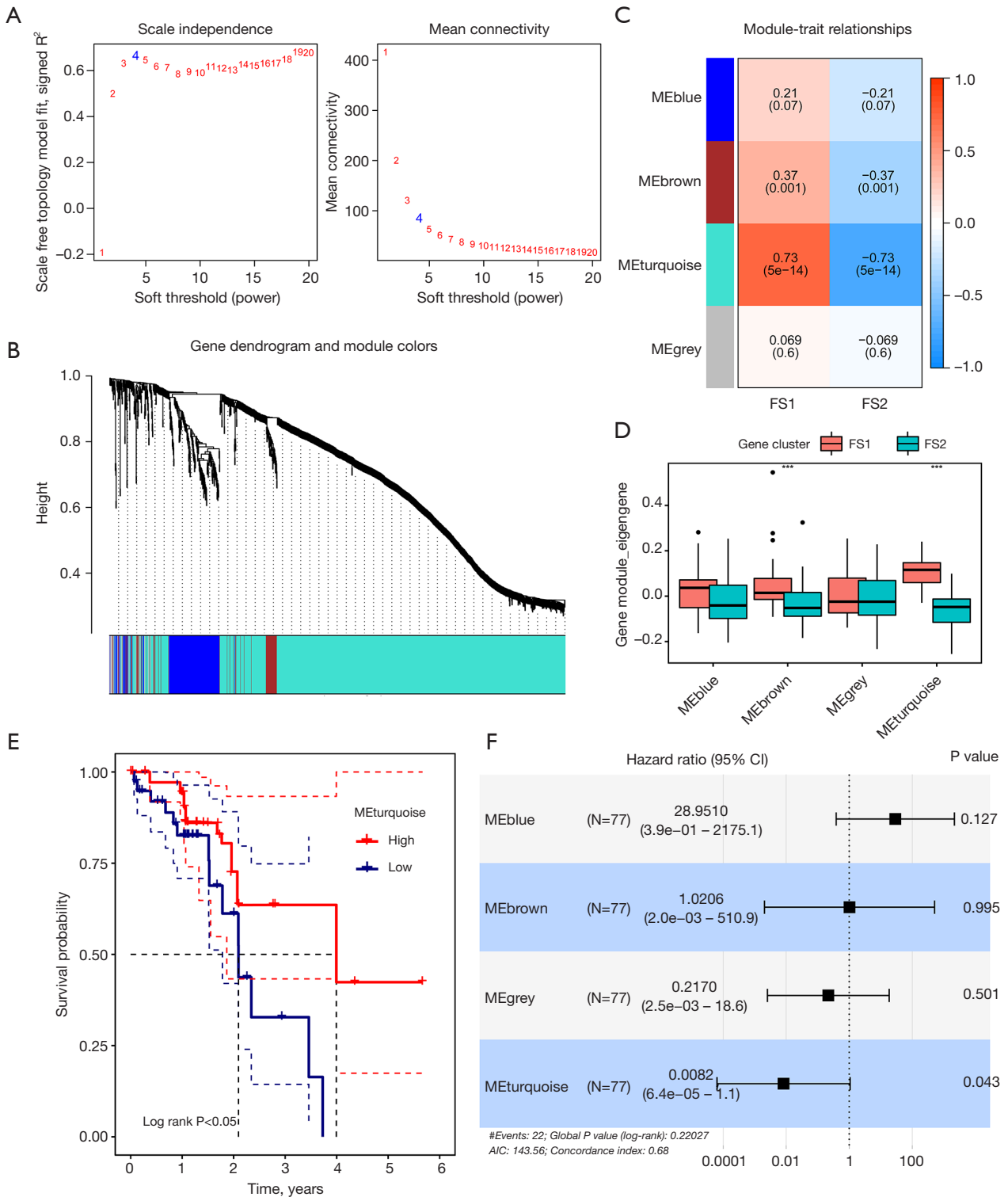


Figure 8 Identification of core genes of ferroptosis. (A-C) The optimal soft threshold of WGCNA (A) and followed obtained 4 modules (B,C). (D) Comparison of different modules of ferroptosis subtypes. (E) Kaplan-Meier of turquoise module. (F) Multivariate Cox regression analysis of different modules. ME, module eigengene; FS1, ferroptosis subtype 1; FS2, ferroptosis subtype 2; AIC, Akaike information criterion; WGCNA, weighted gene co-expression network analysis.

which classified ferroptosis-related genes—namely, *MMD*, *MTDH*, and *TFRC*—into two distinctive subtypes within ESCC. A pivotal aspect of our findings emerged when assessing survival outcomes; strikingly, the FS2 subtype was associated with markedly inferior prognostic trajectories when juxtaposed with its counterpart. This observation incited a subsequent analytical layer involving mutational landscapes and scrutiny of immune-related genetic expressions. In an intriguing twist, the FS2 subtype not only suffered a higher load of gene mutations but also an intensification in immune cell infiltration, with B cells, macrophages, dendritic cells, and other antigen-presenting cohorts being particularly prominent. Such a pattern may well signify an augmented receptivity to immunotherapeutic modalities for the FS2 subtype, an avenue which merits further exploration given the subsisting challenges in treatment stratification for ESCC. Our foray into the ferroptosis milieu within ESCC unearthed a constellation of hub genes within the turquoise module during WGCNA. These hub genes assume a cardinal role in prognostication and are primed for evaluating their utility as biomarkers and as novel contenders for mRNA vaccine targets. Thus, our enriched discussion underscores not only our analytical journey but also crystallizes the conclusions that the patterning of ferroptosis-related genetics holds consequential standing in both prognosis and therapeutic innovation in ESCC. These insights carve a path toward a tailored intervention strategy that may, in time, yield potent armaments in the oncological battle, specifically against ESCC.

MMD corresponds to a gene implicated in the differentiation process of monocytes into macrophages. Presently, research endeavors investigating the association between the *MMD* gene and tumors, particularly in relation to ferroptosis, remain scarce. Prior findings have evinced an elevation in *MMD* expression in lung cancer compared to healthy lung tissue. Furthermore, experimental interventions targeting *MMD* have exhibited a capacity to impede cancer cell line growth, whether in *in vivo* or *in vitro* settings (19). Notably, the miR-140-5p/*MMD* axis has been identified as a modulator of lung cancer cell proliferation through its regulation of the ERK pathway (19). In various malignancies, namely colorectal cancer (20), pancreatic cancer (21), hepatocellular carcinoma (22) and breast cancer (23), prior investigations have demonstrated an augmented expression of *MTDH*. This elevation in expression has been closely implicated in stimulating tumor growth, facilitating metastasis, and fostering resistance to treatment.

Remarkably, interventions targeting this gene have shown potential in reversing drug resistance observed in tumors (20-23). Consistent with our own findings, a thorough analysis of the TCGA and GEO databases revealed *MTDH* as a prospective ferroptosis-related diagnostic gene in hepatocellular carcinoma (24). Furthermore, Bi *et al.* have emphasized that *MTDH* contributes to the susceptibility to ferroptosis through the inhibition of GPX4 and SLC3A2 (25). *TFRC*, encoding transferrin receptor 1, serves as a pivotal iron transporter residing on the cellular membrane. Notably, *TFRC* exhibits pronounced expression in various malignancies (26). This heightened expression promotes tumor proliferation, migration, and transformation of macrophages into the M2 phenotype, thus correlating with unfavorable prognosis. In line with our investigation, *TFRC* mRNA levels positively correlate with ferroptosis in lung cancer (26). Moreover, comprehensive analysis of the TCGA and other relevant databases identified *TFRC* as a potential prognostic gene in prostate cancer, bladder cancer, and other tumors. Additionally, *TFRC* represents a promising antigen for the development of mRNA vaccines in bladder cancer (27,28). As a result, the elevated expression of *MMD*, *MTDH*, and *TFRC* genes, as identified in the screened databases, offers prospects for targeting ferroptosis and holds promise as effective targets for mRNA vaccines.

By conducting cluster analysis on the ferroptosis genes in TCGA-ESCC and GSE53625 data sets, we identified two distinct ferroptosis subtypes, namely FS1 and FS2, which exhibited significant differences in survival outcomes. Notably, the FS2 subtype exhibited a significantly higher total number of TMB and mutations compared to FS1, as well as upregulated expression levels of the ICP and ICD genes. Additionally, an increased presence of immune cells such as CD8⁺ T, CD56, and NKT cells was observed in the FS2 subtype, indicative of a poorer prognosis among patients with high FS2 scores. These findings suggest that FS2 might represent an immunotherapy-sensitive phenotype. In line with previous research on the immune microenvironment of esophageal cancer, our study yielded similar conclusions. Specifically, Ma *et al.* (29) demonstrated a strong correlation between high TMB in esophageal cancer and the shortest distance from tumor cells to APC, as well as improved survival outcomes. Furthermore, a combination of radiotherapy, chemotherapy, and anti-PD-L1 treatment was found to enhance the migration of dendritic cells (DCs) and macrophages towards tumor cells. Another study conducted a systemic analysis of

transcriptional group information from 857 patients with ESCC and protein expression profiles from 124 patients, suggesting a link between ferroptosis and immune activation. Consistent with these findings, our study revealed a higher infiltration of leukocytes, DCs, and macrophages in subtypes exhibiting high ICD expression levels. These results align with previous research in other cancers, demonstrating the potential for classifying different tumors based on ferroptosis gene expression and highlighting the immunotherapy-sensitive phenotypes associated with immune infiltration and TMB (30). Individuals with a significant immune cell infiltration and high TMB exhibited enhanced responsiveness to anti-PD-L1 immunotherapy (30). A separate investigation involving 40 differentially expressed genes associated with ferroptosis in prostate cancer revealed that the high-expression group manifested increased immune cell infiltration, a more favorable tumor immune microenvironment, higher PD-L1 expression, and that the scoring system was particularly applicable to younger patients with T3–4 or N0 stages (31). Wang's team developed a scoring system, utilizing RNA-seq analysis of gliomas and focusing on the expression of ferroptosis-related genes, which identified a resistant-to-ferroptosis high-score group with a worse prognosis (32). Taken together, these findings suggest a correlation between ferroptosis, tumor invasion, and immune cell communication. Based on our own results, we contend that the categorization of ferroptosis subtypes not only aids in predicting patient prognosis but also allows for the identification of individuals more suitable for immunotherapy and tailored medication guidance.

Eventually, we constructed the ferroptosis gene locus in patients diagnosed with ESCC and categorized it into three distinct states. Subsequent analysis revealed significant differences in survival outcomes among the three groups. Through our application of WGCNA, we further stratified the ESCC-associated ferroptosis genes into four distinct modules. Remarkably, the turquoise module emerged as a noteworthy prognostic factor, exhibiting independence in its predictive value. Consequently, several key hub genes were identified within this module, offering potential facilitation for the advancement of mRNA vaccine research and development. In addition to our findings, Zhang *et al.* (33) carried out an analysis on ESCC-associated ferroptosis genes, successfully dividing them into three subtypes. Notably, type C exhibited the most favorable prognosis, accompanied by a superior immune microenvironment score and improved response to anti-PD-L1 treatment. However, no significant

disparities in TMB were observed among the three groups. Furthermore, Zhu *et al.* (34) conducted an analysis on long non-coding RNA in ESCC patients, and indicated that patients deemed high-risk exhibited poorer survival outcomes, unfavorable immune microenvironments, and limited benefits from immunotherapy. Our results indicated that the prognosis of FS2 subtype was inferior to that of FS1. Nonetheless, FS2 demonstrated increased immune infiltration and TMB.

It is important to note that our study possesses certain limitations. Firstly, esophageal cancer exhibits significant geographic variation, with ESCC being more common in Asia, particularly within China. However, due to the relatively small proportion of Asian population within the TCGA and GEO databases, an inclusion of bioinformatics data from Chinese ESCC patients would likely enable more comprehensive and insightful results. Secondly, although we managed to identify several hub genes potentially exploitable for mRNA vaccine development, their practical application remains distant and necessitates further investigation. Specifically, the experimental validation of hub genes for mRNA vaccine development has not been conducted. However, we believe that the findings of this study will lay a solid foundation for future experimental work, and experimental validation of our predictions is an important next step for the progression of this research field.

Conclusions

In this investigation, we conducted a comprehensive analysis of the gene expression profile of ESCC using data from the TCGA and GEO databases. Our examination led to the identification of two distinct subtypes of ferroptosis in ESCC. Subsequently, verification confirmed that the FS2 subtype exhibits a higher frequency of mutations and greater infiltration of immune cells. Furthermore, it demonstrated a more favorable response to immunotherapy, making it a potential effective prognostic marker for esophageal cancer and a prime candidate for targeted immunotherapeutic interventions. These findings provide essential theoretical support for the advancement of mRNA vaccines in the field.

Acknowledgments

We appreciate all the participating patients for their contributions, and the Department of Radiation of Southern Medical University for its support.

Funding: This work was supported by the National Natural Science Foundation of China Grant (No. 82172642 to W.W.).

Footnote

Reporting Checklist: The authors have completed the TRIPOD reporting checklist. Available at <https://tcr.amegroupp.com/article/view/10.21037/tcr-23-2027/rc>

Peer Review File: Available at <https://tcr.amegroupp.com/article/view/10.21037/tcr-23-2027/prf>

Conflicts of Interest: All authors have completed the ICMJE uniform disclosure form (available at <https://tcr.amegroupp.com/article/view/10.21037/tcr-23-2027/coif>). W.W. reports that he has received the support of National Natural Science Foundation of China Grant (No. 82172642) in the present study. The other authors have no conflicts of interest to declare.

Ethical Statement: The authors are accountable for all aspects of the work in ensuring that questions related to the accuracy or integrity of any part of the work are appropriately investigated and resolved. The study was conducted in accordance with the Declaration of Helsinki (as revised in 2013). The current study follows the open-source TCGA and GEO data access policies and publication guidelines. Data can be downloaded for free. There are no ethical issues and informed consent in our study was not required.

Open Access Statement: This is an Open Access article distributed in accordance with the Creative Commons Attribution-NonCommercial-NoDerivs 4.0 International License (CC BY-NC-ND 4.0), which permits the non-commercial replication and distribution of the article with the strict proviso that no changes or edits are made and the original work is properly cited (including links to both the formal publication through the relevant DOI and the license). See: <https://creativecommons.org/licenses/by-nc-nd/4.0/>.

References

- Sung H, Ferlay J, Siegel RL, et al. Global Cancer Statistics 2020: GLOBOCAN Estimates of Incidence and Mortality Worldwide for 36 Cancers in 185 Countries. *CA Cancer J Clin* 2021;71:209-49.
- Siegel RL, Miller KD, Fuchs HE, et al. Cancer Statistics, 2021. *CA Cancer J Clin* 2021;71:7-33.
- Abnet CC, Arnold M, Wei WQ. Epidemiology of Esophageal Squamous Cell Carcinoma. *Gastroenterology* 2018;154:360-73.
- He Y, Li D, Shan B, et al. Incidence and mortality of esophagus cancer in China, 2008-2012. *Chin J Cancer Res* 2019;31:426-34.
- Eyck BM, van Lanschot JJB, Hulshof MCCM, et al. Ten-Year Outcome of Neoadjuvant Chemoradiotherapy Plus Surgery for Esophageal Cancer: The Randomized Controlled CROSS Trial. *J Clin Oncol* 2021;39:1995-2004.
- Teixeira Farinha H, Digkila A, Schizas D, et al. Immunotherapy for Esophageal Cancer: State-of-the Art in 2021. *Cancers (Basel)* 2022;14:554.
- Dixon SJ, Lemberg KM, Lamprecht MR, et al. Ferroptosis: an iron-dependent form of nonapoptotic cell death. *Cell* 2012;149:1060-72.
- Galluzzi L, Vitale I, Aaronson SA, et al. Molecular mechanisms of cell death: recommendations of the Nomenclature Committee on Cell Death 2018. *Cell Death Differ* 2018;25:486-541.
- Viswanathan VS, Ryan MJ, Dhruv HD, et al. Dependency of a therapy-resistant state of cancer cells on a lipid peroxidase pathway. *Nature* 2017;547:453-7.
- Jiang X, Stockwell BR, Conrad M. Ferroptosis: mechanisms, biology and role in disease. *Nat Rev Mol Cell Biol* 2021;22:266-82.
- Chen X, Kang R, Kroemer G, et al. Broadening horizons: the role of ferroptosis in cancer. *Nat Rev Clin Oncol* 2021;18:280-96.
- Chen X, Kang R, Kroemer G, et al. Ferroptosis in infection, inflammation, and immunity. *J Exp Med* 2021;218:e20210518.
- Shui S, Zhao Z, Wang H, et al. Non-enzymatic lipid peroxidation initiated by photodynamic therapy drives a distinct ferroptosis-like cell death pathway. *Redox Biol* 2021;45:102056.
- Xu Z, Tang J. RelB silencing to reverse tamoxifen resistance by regulating GPx4 and ferroptosis in breast cancer. *J Clin Oncol* 2020;38:e12513.
- Inogés S, Tejada S, de Cerio AL, et al. A phase II trial of autologous dendritic cell vaccination and radiochemotherapy following fluorescence-guided surgery in newly diagnosed glioblastoma patients. *J Transl Med* 2017;15:104.
- Lilleby W, Gaudernack G, Brunsvig PF, et al. Phase I/IIa clinical trial of a novel hTERT peptide vaccine in men

- with metastatic hormone-naïve prostate cancer. *Cancer Immunol Immunother* 2017;66:891-901.
17. Liu L, Wang Y, Miao L, et al. Combination Immunotherapy of MUC1 mRNA Nano-vaccine and CTLA-4 Blockade Effectively Inhibits Growth of Triple Negative Breast Cancer. *Mol Ther* 2018;26:45-55.
 18. Nguyen QT, Kwak C, Lee WS, et al. Poly- γ -Glutamic Acid Complexed With Alum Induces Cross-Protective Immunity of Pandemic H1N1 Vaccine. *Front Immunol* 2019;10:1604.
 19. Li W, He F. Monocyte to macrophage differentiation-associated (MMD) targeted by miR-140-5p regulates tumor growth in non-small cell lung cancer. *Biochem Biophys Res Commun* 2014;450:844-50.
 20. Abdel Ghafar MT, Soliman NA. Metadherin (AEG-1/MTDH/LYRIC) expression: Significance in malignancy and crucial role in colorectal cancer. *Adv Clin Chem* 2022;106:235-80.
 21. Chen Z, Ma Y, Pan Y, et al. MiR-1297 suppresses pancreatic cancer cell proliferation and metastasis by targeting MTDH. *Mol Cell Probes* 2018;40:19-26.
 22. Sarkar D. AEG-1/MTDH/LYRIC in liver cancer. *Adv Cancer Res* 2013;120:193-221.
 23. Shen M, Wei Y, Kim H, et al. Small-molecule inhibitors that disrupt the MTDH-SND1 complex suppress breast cancer progression and metastasis. *Nat Cancer* 2022;3:43-59.
 24. Yi S, Zhang C, Li M, et al. Construction of a Novel Diagnostic Model Based on Ferroptosis-Related Genes for Hepatocellular Carcinoma Using Machine and Deep Learning Methods. *J Oncol* 2023;2023:1624580.
 25. Bi J, Yang S, Li L, et al. Metadherin enhances vulnerability of cancer cells to ferroptosis. *Cell Death Dis* 2019;10:682.
 26. Zhang Q, Yi H, Yao H, et al. Artemisinin Derivatives Inhibit Non-small Cell Lung Cancer Cells Through Induction of ROS-dependent Apoptosis/Ferroptosis. *J Cancer* 2021;12:4075-85.
 27. Liu H, Gao L, Xie T, et al. Identification and Validation of a Prognostic Signature for Prostate Cancer Based on Ferroptosis-Related Genes. *Front Oncol* 2021;11:623313.
 28. Gui CP, Li JY, Fu LM, et al. Identification of mRNA vaccines and conserved ferroptosis related immune landscape for individual precision treatment in bladder cancer. *J Big Data* 2022;9:88.
 29. Ma X, Guo Z, Wei X, et al. Spatial Distribution and Predictive Significance of Dendritic Cells and Macrophages in Esophageal Cancer Treated With Combined Chemoradiotherapy and PD-1 Blockade. *Front Immunol* 2022;12:786429.
 30. Zhang W, Yao S, Huang H, et al. Molecular subtypes based on ferroptosis-related genes and tumor microenvironment infiltration characterization in lung adenocarcinoma. *Oncoimmunology* 2021;10:1959977.
 31. Ke ZB, You Q, Sun JB, et al. A Novel Ferroptosis-Based Molecular Signature Associated with Biochemical Recurrence-Free Survival and Tumor Immune Microenvironment of Prostate Cancer. *Front Cell Dev Biol* 2022;9:774625.
 32. Wang Z, Dai Z, Zheng L, et al. Ferroptosis Activation Scoring Model Assists in Chemotherapeutic Agents' Selection and Mediates Cross-Talk With Immunocytes in Malignant Glioblastoma. *Front Immunol* 2022;12:747408.
 33. Zhang LL, Zhu WJ, Zhang XX, et al. Ferroptosis patterns and tumor microenvironment infiltration characterization in esophageal squamous cell cancer. *Front Genet* 2022;13:1047382.
 34. Zhu T, Ma Z, Wang H, et al. Immune-Related Long Non-coding RNA Signature and Clinical Nomogram to Evaluate Survival of Patients Suffering Esophageal Squamous Cell Carcinoma. *Front Cell Dev Biol* 2021;9:641960.

Cite this article as: Zeng Q, Chen B, Wang W. Identification of tumor antigens for mRNA vaccines and ferroptosis-related landscape in esophageal squamous cell carcinoma. *Transl Cancer Res* 2024;13(6):2860-2876. doi: 10.21037/tcr-23-2027